

Antiferromagnetic hysteresis above the spin-flop field

M. J. Grzybowski ^{1,2,*} C. F. Schippers ¹ O. Gomonay ³ K. Rubi ^{4,†} M. E. Bal ⁴ U. Zeitler,⁴ A. Kozioł-Rachwał,⁵ M. Szytma,⁵ W. Janus,⁵ B. Kurowska,⁶ S. Kret,⁶ M. Gryglas-Borysiewicz ² B. Koopmans,¹ and H. J. M. Swagten¹

¹*Department of Applied Physics, Eindhoven University of Technology, PO Box 513, 5600 MB Eindhoven, The Netherlands*

²*Faculty of Physics, University of Warsaw, ul. Pasteura 5, PL-02-093 Warsaw, Poland*

³*Institute of Physics, Johannes Gutenberg-University Mainz, 55128 Mainz, Germany*

⁴*High Field Magnet Laboratory (HFML-EMFL), Radboud University, 6525 ED Nijmegen, The Netherlands*

⁵*Faculty of Physics and Applied Computer Science, AGH University of Science and Technology, 30-059 Kraków, Poland*

⁶*Institute of Physics, Polish Academy of Sciences, Al. Lotników 32/46, PL-02-668 Warsaw, Poland*



(Received 2 September 2021; revised 21 November 2022; accepted 25 January 2023; published 6 February 2023)

Magnetocrystalline anisotropy is essential in the physics of antiferromagnets and commonly treated as a constant, not depending on an external magnetic field. However, we demonstrate that in CoO the anisotropy should necessarily depend on the magnetic field, which is shown by the spin Hall magnetoresistance of the CoO|Pt device. Below the Néel temperature CoO reveals a spin-flop transition at 240 K at 7.0 T, above which a hysteresis in the angular dependence of magnetoresistance unexpectedly persists up to 30 T. This behavior is shown to agree with the presence of the unquenched orbital momentum, which can play an important role in antiferromagnetic spintronics.

DOI: [10.1103/PhysRevB.107.L060403](https://doi.org/10.1103/PhysRevB.107.L060403)

Antiferromagnetic thin-film materials have attracted a lot of attention recently due to their unique properties that create potential applications in spintronics such as data storage [1,2] or long-distance spin transport [3,4]. Their robustness against external magnetic fields is an important promise for using these antiferromagnetic materials. Therefore, they demand strong magnetic fields for reorientation of the spins, and the understanding of the impact of such fields is essential. The behavior of an antiferromagnet (AF) in high magnetic fields is governed by the competition between magnetocrystalline anisotropy and antiferromagnetic exchange interactions. Detailed knowledge of this anisotropy is key to determine possible magnetic configurations of an antiferromagnet as well as proper device design and experimental geometry for potential applications. It is common to treat the anisotropy as a physical parameter that is strictly constant for a given temperature [5–7].

In this letter, we demonstrate that the magnetic anisotropy of a thin-film CoO with adjacent Pt layer can be modified by strong magnetic fields. It manifests itself in the angular dependent magnetoresistance of the CoO|Pt as clear, reproducible and abrupt changes of resistivity coexisting with the hysteresis around the hard axis, which are present up to the highest tested magnetic fields of $B = 30$ T. Such behavior cannot be reproduced by a simple macrospin model nor a domain model. We explain it by the contribution of the unquenched orbital momentum into the anisotropy.

We start with an experimental study of spin reorientation induced by the strong magnetic fields in CoO|Pt. When the

magnetic field \mathbf{B} is applied to an AF along an easy axis, the Néel vector \mathbf{n} , which is the difference of the two sublattice magnetizations, may reorient perpendicularly to the field. It is a well-known spin-flop transition and occurs at the spin-flop field B_{sf} , which depends on the magnetic anisotropy. This reorientation of \mathbf{n} can be detected by the spin Hall magnetoresistance (SMR) [5–9]. The angular dependence of the SMR allows extracting the spin-flop field values for different geometrical configurations of the magnetic field and thus, the intriguing behavior of the anisotropy in CoO can be observed. Here, we show that the spin-flop transition is clearly detected together with a remarkable presence of the hysteretic behavior of the AF. The electrical measurements were performed on Hall bar devices made of a CoO thin film grown on MgO (001) single crystals and capped with 5-nm Pt layer. In the main text we present data for the 2-nm CoO prepared by reactive DC magnetron sputtering (Fig. 1). For validation purposes, other molecular beam epitaxy grown CoO layers, which yielded quantitatively similar results [10], were investigated. Similarly, a reference polycrystalline 5-nm Pt layer was sputtered directly on MgO and examined which is presented in the Supplemental Material [10].

We focus on the analysis of the transverse resistance R_{xy} variations as it can be measured with better accuracy due to the smaller zero-field offset and smaller temperature sensitivity than the longitudinal resistance. The longitudinal data was also analyzed and can be consistently described within the same model [10]. Moreover, a reference device made of MgO|Pt grown and fabricated in an analogous manner has been studied to rule out effects originating from the mere Pt layer [10] such as the Hanle magnetoresistance [11]. All data presented here were collected below the Néel temperature at $T = 240$ K. The background signal coming likely from small sample misalignment with respect to the magnetic field was subtracted [10].

*Michal.Grzybowski@fuw.edu.pl

†Present address: National High Magnetic Field Laboratory, Los Alamos National Laboratory, Los Alamos, New Mexico 87545, USA.

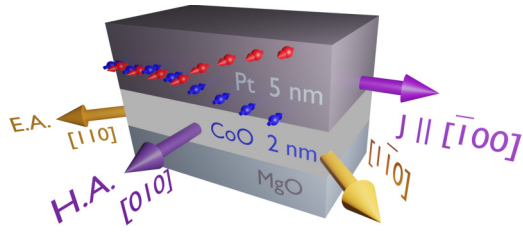


FIG. 1. The scheme of the structure used for the experiments. \mathbf{J} represents the current direction. Magnetic easy (hard) axes are marked by orange (violet) arrows. Blue and red arrows represent the spin accumulation in Pt due to the spin Hall effect.

Initially, the expected in-plane biaxial anisotropy of the CoO thin film with easy axes along $[110]$ and $[\bar{1}\bar{1}0]$ (orange arrows in Fig. 1) is verified [9,12]. To do this, the in-plane magnetic field of 30 T is applied along the expected easy axis $[1\bar{1}0]$ to set a well-defined AF state of $\mathbf{n} \parallel [110]$. Afterwards, the actual field sweep from 0 to 30 T is performed with the fixed orientation of $\mathbf{B} \parallel [110]$ and the resistance is measured (Fig. 2). Upon increasing the magnitude of \mathbf{B} the signal is initially constant and then an abrupt change of R_{xy} can be seen at $B = 7$ T. This significant change appears only when the magnitude of B is increasing. Similar behavior is observed with the magnetic field pointing along another easy axis (see [10]). The abrupt change of R_{xy} does not appear above the Néel temperature [10]. Moreover, it does not correlate with any random fluctuations of temperature. Finally, the probing current density does not change during the experiments, so thermal effects can be ruled out. Therefore, the electrical signal can be attributed to the transverse SMR. The abrupt change of resistance at 7 T reflects the spin-flop transition, where the Néel vector \mathbf{n} changes the orientation from $\mathbf{B} \parallel \mathbf{n}$ to $\mathbf{B} \perp \mathbf{n}$ when B is increasing. The resistance change at the spin flop is consistent with the negative sign of SMR [5,9,13]. Nonlinear behavior of SMR in high fields can originate from progressive spin canting and the occurrence of small net magnetic moment \mathbf{m} as depicted symbolically by double-color arrows in Fig. 2.

To verify the qualitative understanding of the obtained results, we construct a macrospin model. Two magnetic moments coupled antiferromagnetically are considered. The energy expression [14] can be formulated as follows:

$$E(\mathbf{n}) = \frac{2}{B_{sf}^2} (\mathbf{B} \cdot \mathbf{n})^2 - (n_x^4 + n_y^4) + \frac{B_{an\parallel}}{B_{an\perp}} n_z^2. \quad (1)$$

In-plane biaxial anisotropy field and out-of-plane uniaxial anisotropy field are represented by $B_{an\perp}$ and $B_{an\parallel}$, respectively. The two orthogonal easy directions in-plane are denoted as x, y and correspond to $[110]$ and $[\bar{1}\bar{1}0]$, respectively (Fig. 1). The spin-flop field is denoted by B_{sf} and equals $B_{sf} = 2\sqrt{B_{ex}B_{an\perp}}$ [14], where B_{ex} is the exchange field. The value of B_{sf} is determined from the experimental data (Fig. 2). \mathbf{B} remains in the plane of the sample in all experiments. The spins are expected to remain in-plane due to thin-film character of the sample [9,12] and the out-of-plane anisotropy field is set $B_{an\parallel} \gg B_{an\perp}$. We perform the energy minimization with B_{sf} and coordinates of \mathbf{B} as the only parameters, from which we obtain the expected orientation of \mathbf{n} . With the assumption of $B \ll B_{ex}$, the magnitude of finite \mathbf{m} perpendicular to \mathbf{n} due to the tilt of the spin sublattices

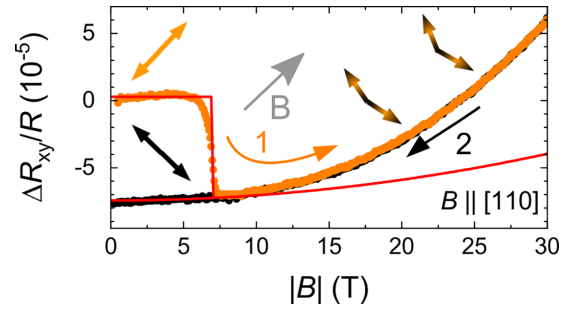


FIG. 2. Transverse magnetoresistance for the CoO|Pt structure collected for increasing (orange points) or decreasing (black points) B along the $[110]$ easy axis. The order of the measurements is indicated by the digits. The expected shape of the SMR signal calculated within the macrospin model for $B_{sf} = 7.0$ T is presented by the red curve. The thick arrows represent the directions of the spins (spin canting, angle not to scale) with respect to the magnetic field (thin grey arrow). The electrical signal is expressed as $\Delta R_{xy}/R$, where ΔR_{xy} is the difference in resistance between a data point taken in a magnetic field and the initial value $R_{xy}(B = 0)$. Sheet resistance averaged over different magnetic fields is denoted by R .

can be estimated [10,14]. The SMR signal can be modeled by $R_{xy} \propto \rho_n n_{\parallel} n_{\perp} + \rho_m m_{\parallel} m_{\perp}$. For qualitative analysis, it is enough to approximate the ratio between ρ_n and ρ_m [10]. Even when allowing for the possibility that SMR probes not only the spin part but rather the total the angular momentum this would not influence the position of the sharp resistance transition and the hysteresis. Therefore, whatever component contributes to the signal, the hysteresis width would be the same for both the spin and the orbital component.

Comparison of the model to the field sweep along $[110]$ presented in Fig. 2 reveals good qualitative agreement. It should be noted that the quantitative difference between the model and data can be explained by the fact that we deal with a domain structure and only part of the domains are initially oriented parallel to the field. Therefore, the magnitudes of the abrupt resistance change at 7 T and the progressive resistance increase for $B > 7$ T cannot be easily captured by the simple macrospin model.

Despite a good correlation between the model and the experimental data for the field along an easy direction, we find that the model cannot describe the measurements for the magnetic field along a hard axis [10]. To clarify it, we perform an angular dependent magnetoresistance (ADMR) measurements at different magnetic fields and show the data for $B = 10$ T and $B = 25$ T in Fig. 3. These angle-dependent measurements determine how \mathbf{n} evolves upon gradually changing the magnetic field of a fixed magnitude from an easy to a hard axis. The resistance is recorded as a function of an angle α between the magnetic field and $[010]$, which is a hard axis. Above the $B_{sf} = 7$ T, \mathbf{n} is expected to follow the direction perpendicular to \mathbf{B} , which is high enough to overcome the in-plane anisotropy [7]. This should be reflected in the SMR signal that is shown as the green dashed lines in Fig. 3, which is the result of the macrospin model calculation with experimentally determined B_{sf} .

Remarkably, the experiments show a completely different SMR dependence. When the magnetic field changes the

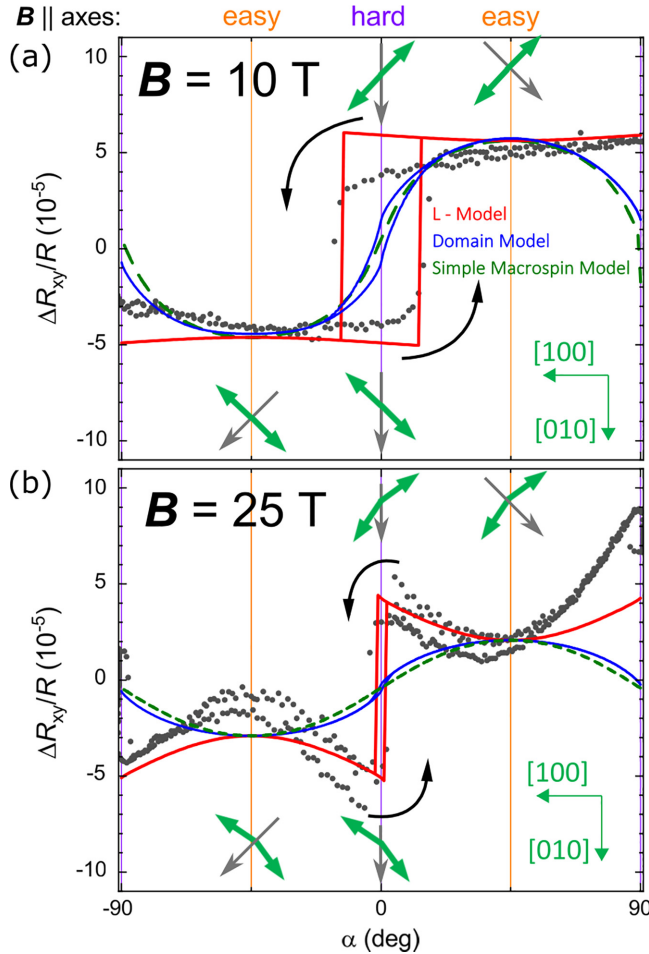


FIG. 3. The angular dependence of magnetoresistance for the CoO structure collected at (a) $B = 10$ T and (b) $B = 25$ T is depicted by the black dots compared with the simple macrospin model (green dashed line), domain model (blue line) and L model with $\xi = -4.02$ (red line). The experimental data are expressed as relative changes of the resistance as a function of an angle α . Green (gray) arrows represent the spin (magnetic field) orientation with respect to crystalline axes (coordinates in bottom right corner). Black arrows depict the angle sweeping direction.

orientation from $\alpha = 90^\circ$ to $\alpha = -90^\circ$ and back, the electrical signal follows the same trend except for the region close to $\alpha = 0^\circ$. In the vicinity of $\alpha = 0^\circ$, the point where the magnetic field points along the hard axis, the SMR shows a hysteresis loop (Fig. 3). At higher magnetic fields, the hysteresis becomes narrower. The hysteresis can be characterized by its width and plotted as a function of \mathbf{B} (Fig. 4). Then, it can be clearly seen that hysteresis loops appear in the whole range of tested magnetic fields between B_{sf} up to 30 T. The hysteresis loops are absent above T_N and thus they can be attributed to the antiferromagnetic behavior of CoO. Below B_{sf} , no abrupt resistance changes are detectable and only slight residual hysteretic behavior around $\alpha = 0$ can be observed that can be due to possible domain structure in the system [10]. The experimental results can be understood as the Néel vector lagging behind the magnetic field due to the strong in-plane anisotropy. However, such an effect is expected only

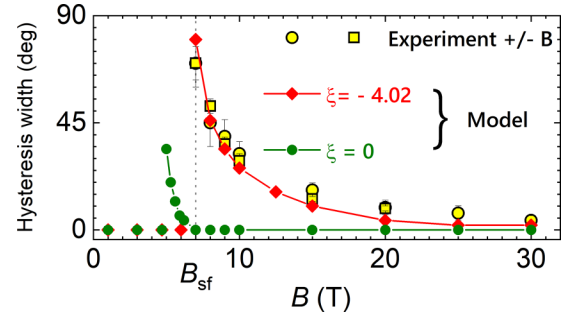


FIG. 4. Summary of the hysteresis width observed in ADMR as a function of the magnetic field (yellow squares and circles) compared to the simple macrospin model ($\xi = 0$, green circles) and L model with $\xi = -4.02$ (red diamonds). Lines are guides for the eye.

below B_{sf} , but should be absent above the spin-flip in our current understanding of the interplay between Zeeman energy, antiferromagnetic exchange, and anisotropy energy, where \mathbf{n} should follow the direction perpendicular to the magnetic field [7].

First, we check whether the existence of a domain structure can explain the experimental observations. We consider a set of Néel vectors that experience different anisotropy fields which reflects possible inhomogeneity of the layer that can result in antiferromagnetic domains. We simulate an ADMR measurement for each case separately using Eq. (1) and average obtained results assuming a Gaussian distribution of the spin-flip fields centered around 7 T [10]. We refer to this as a domain model [10]. As can be seen in the blue line in Fig. 3 such a procedure can indeed result in appearance of a small hysteresis in ADMR above the spin-flip field. However, it completely fails to reproduce the abrupt transitions visible in strong magnetic fields [Fig. 3(b)] and is therefore not appropriate to explain this observation.

Therefore, we consider another approach to interpret the experimental data. We assume that the magnetic field modifies the magnetic anisotropy of the antiferromagnet. We describe this contribution by introducing an additional, phenomenological energy term, relevant above B_{sf} :

$$E_a = \frac{\xi}{B_{sf}^2} B_x B_y n_x n_y \quad (2)$$

into Eq. (1) with a coefficient ξ . It appears only if the magnetic field has nonzero components for both easy directions. Thus, it follows the symmetry of the experimental observations and can describe the unexpected hysteretic behavior of the AF when a strong magnetic field is parallel to a hard direction. For negative ξ , such a contribution enhances the energy barrier between the states with different orientations of the Néel vector seen as an enhancement of the effective anisotropy field. We believe that this contribution originates from the field-induced tilting of the orbital momentum from the easy axis; and hence we call it the L model.

The existence of the hysteresis loop in SMR can be reproduced using the L model with $\xi = -4.02$ as demonstrated by the solid red lines in Fig. 3. Good agreement of the hysteresis width between the model and experiments is obtained for all magnetic fields tested experimentally (Fig. 4). Slight

deviations from the model that can be seen in the experimental data in Fig. 3(a) as a rounded shape of the hysteresis loop and a difference in the curvature near $\alpha = \pm 45^\circ$ can be interpreted either as a signature of a domain structure and magnetic inhomogeneity of the system (these are also the features of the blue, domain model curve) or the contribution of the angular momentum into the SMR signal. For the model with $\xi = 0$, which corresponds to the original equation (1) and constant magnetic anisotropy, no hysteresis above the B_{sf} is expected as indicated by green dashed lines in Fig. 3 as well as green circles in Fig. 4.

A likely explanation for the observed hysteretic behavior and the additional energy term E_a [Eq. (2)] is the unquenched orbital momentum that is known to be present in CoO and has a strong contribution to the magnetocrystalline anisotropy in this material [15,16]. It has also been observed to manifest itself in the magnon spectrum [17]. Furthermore, the orbital part of the angular momentum L has already been shown to determine the angular magnetoresistance of CeSb, which is a $4f$ monpnictide with unquenched L [18]. In general, it is observed that the orbital part can induce a wide variety of transport phenomena [19], which belong to the most recent discipline of orbitronics.

In our study, we restrict our discussion to the simplest case to qualitatively justify the orbital momentum dependence on the magnetic field and its influence on the anisotropy. First, we note that spin-orbit coupling induces an antiparallel alignment of the effective $L = 1$ orbital angular momenta \mathbf{L}_1 and \mathbf{L}_2 to the corresponding magnetic spins for each sublattices [17]. The external magnetic field $B \leq B_{sf}$ aligned parallel to the magnetic spins does not change this configuration; the orbital angular momenta are aligned antiparallel to spins with $L_{xj} = \pm 1$ (where the quantization axis x is parallel to the easy axis). However, the magnetic field, oriented generically in the xy plane, induces mixing of the states with the projections $L_{jx} = \pm 1$, and 0. This mixing, in turn, results in a nonzero expectation values of quadrupolar variables, $\langle \hat{L}_{jx} \hat{L}_{jy} \rangle$ ($j = 1, 2$) and additional spin anisotropy $K_{an}^{ha} A_{xy}(\mathbf{B}) n_x n_y$ with $A_{xy}(\mathbf{B}) = \sum_{j=1,2} \langle \hat{L}_{jx} \hat{L}_{jy} \rangle$.

To calculate the quantum states of the orbital momenta we introduce the Hamiltonian [17]:

$$\hat{\mathcal{H}} = \sum_{j=1,2} [-K^L (\hat{\mathbf{L}}_j \mathbf{e}_j)^2 + \lambda \mathbf{S}_j \hat{\mathbf{L}}_j + 2\mu_B \mathbf{B} \hat{\mathbf{L}}_j], \quad (3)$$

where K^L is anisotropy of the angular momentum, the constant λ parametrizes spin-orbit coupling, and μ_B is the Bohr magneton. We assume that the orientation of the Néel vectors is fixed along x and the local quantization axes \mathbf{e}_j are parallel/antiparallel to the Néel vector ($\mathbf{e}_1 \uparrow \downarrow \mathbf{e}_2 \uparrow \uparrow \hat{x}$). Figure 5 shows the field dependence of $A_{xy}(\mathbf{B})$ (see the Supplemental Material for more details). Below the critical field (red line), $A_{xy}(\mathbf{B})$ is close to zero, as the quadrupoles $\langle \hat{L}_{1x} \hat{L}_{1y} \rangle$ and $\langle \hat{L}_{2x} \hat{L}_{2y} \rangle$ have opposite signs and almost compensate each other. However, close to the critical field value, the magnetic field is large enough to align both orbital momenta parallel to the magnetic field, and both quadrupoles have the same sign. This induces a rapid increase of $A_{xy}(\mathbf{B})$ above the critical field with the maximum anisotropy value achieved for the field parallel to the hard axis. There is a nonlinear dependence

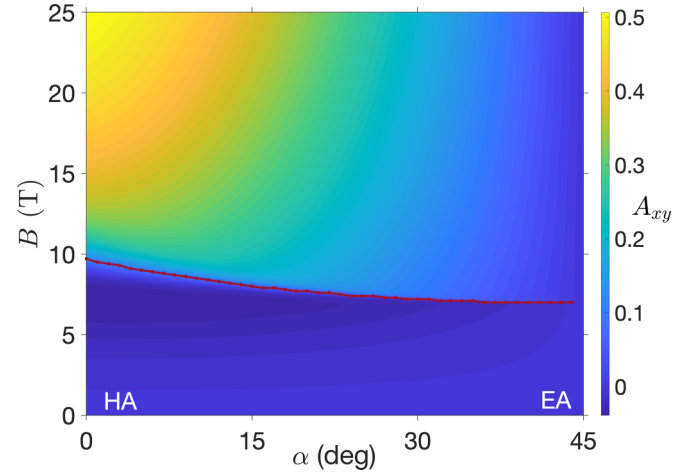


FIG. 5. The value of the field-induced anisotropy $A_{xy}(\mathbf{B}) \equiv \sum_{j=1,2} \langle \hat{L}_{jx} \hat{L}_{jy} \rangle$ (color code, dimensionless) as a function of the orientation and the magnitude of the magnetic field. The star line shows the value of the threshold field $B_{th}(\alpha)$ below which the field-induced anisotropy is negligible. The HA and EA denote a hard and an easy axis, respectively.

of $A_{xy}(\mathbf{B})$ on the magnetic field [10] above the critical field, which we substitute with the B^2 relation for simplicity in our phenomenological energy term [Eq. (2)]. The value of the critical field scales with spin-orbit coupling λ and corresponds to the spin-flop field B_{sf} if \mathbf{B} is parallel to an easy axis. Field-induced rotation of orbital states can induce additional strain $u_{xy} \propto A_{xy}$ that through a magnetoelastic mechanism contributes into effective magnetic anisotropy. We conjecture that a direct experimental confirmation of such behavior of the angular momentum could be performed, for example, by studying the magnetic field induced frequency shift of the magnon modes with optical excitation. We also notice a similarity of the considered case to the Pashen-Back effect, in which the magnetic field is much stronger than the spin-orbit coupling of a system [20].

To summarize, we report the observation of the hysteresis loops in the angular dependence of magnetoresistance of a thin film of CoO with adjacent Pt layer. The hysteretic behavior is unexpectedly present above the spin-flop field and persists up to the highest tested magnetic fields (30 T). It can be interpreted by the dependence of the magnetic anisotropy on the external magnetic field. The unquenched orbital angular momentum is a likely reason for the observed effects. These findings highlight the role of the anisotropy variations induced by the magnetic field and the role of the unquenched orbital momentum in the physics of antiferromagnets and their potential applications.

We thank R. Duine, R. Lavrijsen, M. Baj, and T. Dietl for helpful discussions. We acknowledge P. Lueb and J. Dedding for the VSM-SQUID measurements. This work was supported by HFML-RU/NWO-I, member of the European Magnetic Field Laboratory (EMFL), and by the Ministry of Education and Science, Poland (Grant No. DIR/WK/2018/07) via its membership to the EMFL. Sample fabrication was performed using NanoLabNL facilities. The research was funded

by the Dutch Research Council (NWO) under Grant No. 680-91-113. O.G. acknowledges support from the Alexander von Humboldt Foundation, the ERC Synergy Grant SC2 (No. 610115), and the Deutsche Forschungsgemeinschaft

(DFG, German Research Foundation)–TRR 173–268565370 (Project No. B12). This research was funded in part by National Science Centre, Poland 2021/40/C/ST3/00168.

-
- [1] P. Wadley, B. Howells, J. Zelezny, C. Andrews, V. Hills, R. P. Campion, V. Novak, K. Olejnik, F. Maccherozzi, S. S. Dhesi, S. Y. Martin, T. Wagner, J. Wunderlich, F. Freimuth, Y. Mokrousov, J. Kune, J. S. Chauhan, M. J. Grzybowski, A. W. Rushforth, K. W. Edmonds *et al.*, Electrical switching of an antiferromagnet, *Science* **351**, 587 (2016).
- [2] T. Jungwirth, X. Marti, P. Wadley, and J. Wunderlich, Antiferromagnetic spintronics, *Nat. Nanotechnol.* **11**, 231 (2016).
- [3] R. Lebrun, A. Ross, S. A. Bender, A. Qaiumzadeh, L. Baldrati, J. Cramer, A. Brataas, R. A. Duine, and M. Kläui, Tunable long-distance spin transport in a crystalline antiferromagnetic iron oxide, *Nature (London)* **561**, 222 (2018).
- [4] J. Han, P. Zhang, Z. Bi, Y. Fan, T. S. Safi, J. Xiang, J. Finley, L. Fu, R. Cheng, and L. Liu, Birefringence-like spin transport via linearly polarized antiferromagnetic magnons, *Nat. Nanotechnol.* **15**, 563 (2020).
- [5] G. R. Hoogeboom, A. Aqeel, T. Kuschel, T. T. M. Palstra, and B. J. van Wees, Negative spin Hall magnetoresistance of Pt on the bulk easy-plane antiferromagnet NiO, *Appl. Phys. Lett.* **111**, 052409 (2017).
- [6] L. Baldrati, A. Ross, T. Niizeki, C. Schneider, R. Ramos, J. Cramer, O. Gomonay, M. Filianina, T. Savchenko, D. Heinze, A. Kleibert, E. Saitoh, J. Sinova, and M. Kläui, Full angular dependence of the spin Hall and ordinary magnetoresistance in epitaxial antiferromagnetic NiO(001)/Pt thin films, *Phys. Rev. B* **98**, 024422 (2018).
- [7] S. Geprägs, M. Opel, J. Fischer, O. Gomonay, P. Schwenke, M. Althammer, H. Huebl, and R. Gross, Spin Hall magnetoresistance in antiferromagnetic insulators, *J. Appl. Phys.* **127**, 243902 (2020).
- [8] J. Fischer, O. Gomonay, R. Schlitz, K. Ganzhorn, N. Vlietstra, M. Althammer, H. Huebl, M. Opel, R. Gross, S. T. B. Goennenwein, and S. Geprägs, Spin Hall magnetoresistance in antiferromagnet/heavy-metal heterostructures, *Phys. Rev. B* **97**, 014417 (2018).
- [9] L. Baldrati, C. Schmitt, O. Gomonay, R. Lebrun, R. Ramos, E. Saitoh, J. Sinova, and M. Kläui, Efficient Spin Torques in Antiferromagnetic CoO/Pt Quantified by Comparing Field-And Current-Induced Switching, *Phys. Rev. Lett.* **125**, 077201 (2020).
- [10] See Supplemental Material at <http://link.aps.org/supplemental/10.1103/PhysRevB.107.L060403> for details on layers growth, devices fabrication, experimental procedures, analysis of the results and parameters used for the modelling.
- [11] S. Vélez, V. N. Golovach, A. Bedoya-Pinto, M. Isasa, E. Sagasta, M. Abadia, C. Rogero, L. E. Hueso, F. S. Bergeret, and F. Casanova, Hanle Magnetoresistance in Thin Metal Films with Strong Spin-Orbit Coupling, *Phys. Rev. Lett.* **116**, 016603 (2016).
- [12] W. N. Cao, J. Li, G. Chen, J. Zhu, C. R. Hu, and Y. Z. Wu, Temperature-dependent magnetic anisotropies in epitaxial Fe/CoO/MgO(001) system studied by the planar Hall effect, *Appl. Phys. Lett.* **98**, 262506 (2011).
- [13] H. Nakayama, M. Althammer, Y.-T. Chen, K. Uchida, Y. Kajiwara, D. Kikuchi, T. Ohtani, S. Geprägs, M. Opel, S. Takahashi, R. Gross, G. E. W. Bauer, S. T. B. Goennenwein, and E. Saitoh, Spin Hall Magnetoresistance Induced by a Nonequilibrium Proximity Effect, *Phys. Rev. Lett.* **110**, 206601 (2013).
- [14] H. V. Gomonay and V. M. Loktev, Spin transfer and current-induced switching in antiferromagnets, *Phys. Rev. B* **81**, 144427 (2010).
- [15] J. Kanamori, Theory of the magnetic properties of ferrous and cobaltous oxides, I, *Prog. Theor. Phys.* **17**, 177 (1957).
- [16] J. Kanamori, Theory of the Magnetic properties of ferrous and cobaltous oxides, II, *Prog. Theor. Phys.* **17**, 197 (1957).
- [17] T. Satoh, R. Iida, T. Higuchi, Y. Fujii, A. Koreeda, H. Ueda, T. Shimura, K. Kuroda, V. I. Butrim, and B. A. Ivanov, Excitation of coupled spin-orbit dynamics in cobalt oxide by femtosecond laser pulses, *Nat. Commun.* **8**, 638 (2017).
- [18] J. Xu, F. Wu, J.-K. Bao, F. Han, Z.-L. Xiao, I. Martin, Y.-Y. Lyu, Y.-L. Wang, D. Y. Chung, M. Li, W. Zhang, J. E. Pearson, J. S. Jiang, M. G. Kanatzidis, and W.-K. Kwok, Orbital-flop induced magnetoresistance anisotropy in rare earth monpnictide CeSb, *Nat. Commun.* **10**, 2875 (2019).
- [19] D. Go, D. Jo, H.-W. Lee, M. Kläui, and Y. Mokrousov, Orbital currents in solids, *Europhys. Lett.* **135**, 37001 (2021).
- [20] L. D. Landau and E. M. Lifshitz, *Quantum Mechanics Non-Relativistic Theory* (Pergamon Press, London, 1958).